First publ. in: Journal of Chemical Physic 99 (1993), 4, pp. 3030-3036

Structurally determined Brownian dynamics in ordered colloidal suspensions: Self-diffusion in fluid, supercooled, and crystalline phases

R. Simon, T. Palberg, and P. Leiderer
Fakultät für Physik, Universität Konstanz, W-7750 Konstanz, Federal Republic of Germany

(Received 11 December 1992; accepted 4 May 1993)

Electrostatically interacting colloidal suspensions at medium to very low salt concentrations were prepared in differently ordered phases using the method of continuous deionization. Equilibrium phase states include fluid, mono- and polycrystalline material as well as coexistence between fluid and monocrystal. A nonequilibrium supercooled fluid state is reproducibly reached by shear melting. In these phases the long time self-diffusion coefficient D_L was measured by forced Rayleigh scattering, while the potential of interaction was systematically varied by changing salt concentration c_s and volume fraction ϕ. In the equilibrium fluid D_L decreases by roughly an order of magnitude as the interaction increases. This trend extends continuously into the supercooled state. In all cases crystallization is observed for $D_L/D_0 \leqslant 0.10(1)$. In the polycrystalline phases self-diffusion coefficients are still 1 to 2 orders of magnitude lower than in the supercooled state. Here self-diffusion increases with increasing interaction. For the monocrystalline case upper limits of D_L are given. These data on the solid phases are discussed in terms of grain boundary and vacancy diffusion.

I. INTRODUCTION

Model suspensions of monodisperse spherical particles are ideally suited for investigating the Brownian motion in colloidal suspensions. Each colloidal particle is continuously subjected to collisions with the molecules of the suspending medium, which drive its diffusive motion and also generate a friction depending on the particle size. This is described in terms of the Stokes–Einstein diffusion coefficient

$$D_0=\frac{k_BT}{6\pi\eta r}, \qquad (1)$$

where k_B is the Boltzmann constant, T the temperature, η the viscosity, and r the radius of a spherical particle. The ratio r^2/D_0 sets a natural time scale for the dynamics of a colloidal system.

Recently there has been renewed interest in Brownian dynamics[1] and the current prospect is based on the convergence of several activities: Model colloidal systems were synthesized with well characterized particle geometry and interparticle interactions; advanced light scattering techniques opened access to the relevant time and length scales; the application of theoretical concepts of statistical physics was aided by powerful computational means.

The most important *direct* interparticle interactions are based on Yukawa or screened Coulomb type potentials. In principle the strength and range of interaction may be varied by the particle volume fraction ϕ and the screening parameter within the limiting cases of a hard sphere system[2] and a one component macrofluid.

The presence of these strong direct interactions allows for the study of altered Brownian dynamics in highly correlated, ordered systems. In contrast to disordered systems we now have to discriminate between the behavior on short and on long time scales. For short times the particle diffuses undisturbed by the presence of its neighbors. Hence the short time self-diffusion coefficient D_S equals the Stokes–Einstein value D_0 (1). For long time scales, however, diffusion is significantly hindered by the cage of neighboring particles. A long time self-diffusion coefficient D_L results, with $D_L < D_0$ depending on the strength and range of direct interactions. Short and long times are distinguished by the structural relaxation time τ_r of the cage.

In addition to direct interactions *hydrodynamic* interactions become increasingly important for elevated volume fractions $\phi > 0.01$. Due to these indirect interactions both self-diffusion coefficients D_S and D_L are substantially modified. The theoretical calculations on the influence of hydrodynamic interactions[3–6] are confirmed by a large body of experimental investigations.[1,7–12]

In this paper we are concerned with sufficiently dilute systems, that direct interaction and structural effects solely dominate the long time dynamics and hydrodynamic interaction can savely be neglected.

In the absence of hydrodynamic interactions the long time self-diffusion coefficient of colloidal fluids was shown to be dependent on the radial distribution function $g(r)$ which in turn depends only on the direct interaction potential.[13] This situation can be realized experimentally by using electrostatically interacting particles at $\phi < 0.02$ in combination with very low concentrations c_s of screening salt. Up to now the only systematic measurement on monodisperse low volume fraction systems has been the pioneering work of Dozier and Chaikin.[14] These authors demonstrated that for the named region of volume fractions forced Rayleigh scattering (FRS) is ideally suited for the measurement of long time self-diffusion coefficients of colloidal particles. Only very recently a new deionization technique was reported, which allows to prepare suspensions at extremely low but controlled salt concentrations.[15] In fact the overall ion concentration is only limited by the number of dissociated surface charge groups of the particle; i.e., $c_s = 0$.

The effect of employing this technique in self-diffusion measurements using FRS is twofold: First, we considerably extend the range of self-diffusion measurements in highly correlated, ordered systems. Whereas dynamic light scattering is confined to very low volume fractions due to multiple scattering, former FRS experiments, though being insensitive to multiple scattering, had access to colloidal solids only in a range of volume fractions where hydrodynamic interactions could not be neglected.

The second effect is the reproducible access to differently ordered systems at equal suspension parameters. For example, while the equilibrium phase is a bcc crystal, the preparation process of continuous deionization leaves the suspension in the metastable shear molten state, which solidificates in different morphologies, depending on the details of the preceding shear process and of the nucleation mechanism.[16] Thus we gain access to nonequilibrium fluid states, may discriminate the influence of different crystal morphologies and furthermore study for the first time systematically the crystal size[17] dependence of D_L.

Both the formation of a specific crystal structure and morphology and the self diffusional properties of these low volume fraction suspensions are governed by the direct interparticle interactions. We may describe those in terms of a screened Coulomb potential between two particles of radius a at a distance r

$$U(r)=\frac{Z^2e^2}{4\pi\epsilon_0\epsilon_r}\left\{\frac{\exp(\kappa a)}{1+\kappa a}\right\}^2\frac{\exp(-\kappa r)}{r}, \tag{2}$$

where Ze is the particle charge, ϵ_0, ϵ_r the vacuum permittivity and the dielectric constant of the suspending medium, respectively. The inverse Debye screening length κ depends on the concentration of counterions, i.e., particle concentration n_P times charge number Z, and on the concentration n_i and charge z_i of added salt ions

$$\kappa^2=\frac{e^2}{\epsilon_0\epsilon_r k_B T}\left\{n_P Z+\sum_i n_i z_i^2\right\}. \tag{3}$$

For the limit $a\to 0$ the potential of interaction in Eq. (2) becomes the Yukawa potential.

For interaction energies high compared to thermal energies the charge number Z and inverse screening length κ are to be replaced by their somewhat smaller renormalized values Z^*, κ^*.[18,19] Using this pair interactions equilibrium phase diagrams have been calculated[20–22] showing fluid, bcc, fcc phases, and the respective coexistence regimes, which were found to agree well with experimental data.[23,24] Many aspects of crystallized systems have been studied,[25] but it has been only very recently that also the influence of crystal morphologies has gained considerable interest.[26]

In this paper the diffusional properties in dependence on the sample's morphology are of particular interest. We therefore first present a sketch of our methods to prepare samples of different morphology. We proceed with a short outline of the method of forced Rayleigh scattering. We will then discuss our results in detail for fluid and crystalline phases. Finally we dwell on the possibilities of measuring D_L in coexisting fluid and solid phases.

II. EXPERIMENT

A. Particles

Experiments were performed using polystyrene latex spheres (2011M9R, Seradyn, USA) of hydrodynamic diameter $\sigma_h=102(5)$ nm at volume fractions $\phi\leqslant 0.005$. In good agreement with the data supplied by the manufacturer we find a total number of 3.3×10^4 acid groups per particle, of which 920(20) are strong acid groups.[15] From the latter figure a renormalized charge of $Z^*=510$ is calculated using the model of Alexander *et al.*[18] This calculated charge is of the same order as experimentally determined renormalized charges with $Z^*\approx 400$.[27]

In order to carry out the FRS measurements the particles were treated with a solution of a spiropyrane dye in *p*-xylene.[28] Subsequent evaporation of the xylene left some 2×10^3 dye molecules in the particles. Care was taken that neither the radius nor the charge was influenced by this procedure. The dye is transparent in its ground state. Upon irradiation with ultraviolet light ($\lambda<380$ nm) it is excited into a state absorbing red light. The relaxation from this state back to the ground state is characterized by a function $f_{\mathrm{DYE}}(t)$, which is roughly exponential with a relaxation time of $\tau_{\mathrm{DYE}}\approx 20$ s.

B. Preparation

Suspensions of carefully controlled particle and salt concentrations were prepared using Continuous Deionization.[15] The suspension is pumped peristaltically through a tubing system connecting the ion exchange chamber to the different measuring cells for conductivity, particle concentration and FRS. Before the actual FRS measurements the pump is switched off and the tubes which connect the measuring cell are clamped by electromagnetic valves. Measurements undisturbed by the convective flow in the cell can be started about 5 s after clamping.

For completely deionized suspensions of the described particles the freezing starts at a volume fraction of $\phi_{\mathrm{freeze}}=0.0016(1)$; i.e., by varying the volume fraction between $\phi=0.0005$ and $\phi=0.005$ we are in the fluid and in the bcc region of the equilibrium phase diagram.[24,29] We note that an equilibrium colloidal solid ($\phi>0.0016$) is brought into a metastable, shear molten state, while it is pumped.[30] It readily crystallizes when the flow is stopped. For our cell geometry ($1\times10\times40$ mm) oriented single crystals may be grown after steadily shearing the suspension employing constant hydrostatic pressure differences between two reservoirs[16] refilled by the pump. If the interparticle interaction is not too strong, homogenous nucleation is rare,[33] and twinned single crystals grow from the walls once the shear process has been stopped smoothly. The twin domains are about 100 μm in size,[16] their [111] directions are aligned along the flow direction while their (110) layers are parallel to the cuvette wall. For these twinned single crystals we use the term *monocrystal*. In our experiments oscillatory shearing at low flow rates yielded polycrystalline solids.

Thus different morphologies could be prepared within our experimental setup. Consequently, static light scatter-

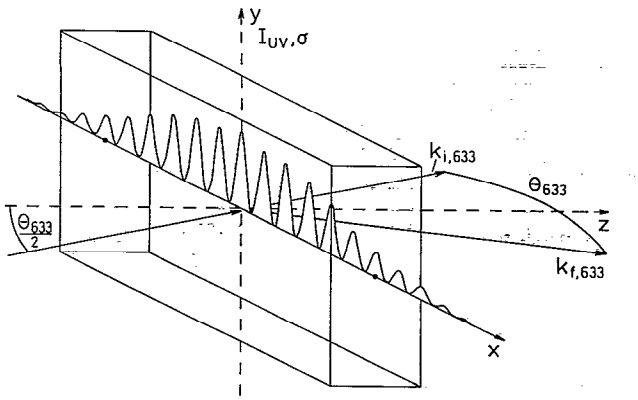

FIG. 1. Schematic sketch of the FRS experiment: Along the x axes, parallel to the long side of the measuring cell, the absorption grid $\sigma(x)$ is proportional to the uv intensity grid $I_{uv}(x)$. Also shown is the scattering geometry for the He–Ne laser beam: $\mathbf{k}_{i,633}$ and $\mathbf{k}_{f,633}$ are the wave vectors of incident and diffracted light, respectively. They obey the diffraction rule $\mathbf{k}_{i,633}-\mathbf{k}_{f,633}=\mathbf{q}$.

ing was performed at the FRS measuring spot to precisely determine the structure and morphology of the individual samples.[16]

C. Forced Rayleigh scattering

The long time self-diffusion coefficient D_L was measured by means of forced Rayleigh scattering.[34–37] Ultraviolet light of $\lambda=351$ nm of an argon ion laser is split into two coherent beams. These are crossed under an angle θ_{uv} in the flat FRS cell filled with the sample of refractive index n to produce a standing interference pattern with wave vector $\mathbf{q}$ parallel to the x direction; i.e., to the cell walls. The magnitude of $\mathbf{q}$ is given by

$$q\equiv|\mathbf{q}|=\frac{4\pi}{n\lambda_{uv}}\sin(\theta_{uv}/2). \tag{4}$$

The sinusoidal modulation of uv intensity leads to an equally sinusoidal excitation of dyed particles into the absorbing state and thus to an absorption grid of wave vector $\mathbf{q}$ (Fig. 1). For the experiments presented here the exposure time was limited to a few milliseconds to optimize the contrast.

Due to self-diffusion of the particles the amplitude of the absorption grid decays with time. In the long time limit, $t>\tau_R$, the mean square displacement $\langle R^2\rangle$ is proportional to t and the long time self-diffusion coefficient D_L. The amplitude σ of the absorption modulation therefore decreases according to a simple exponential law

$$\sigma(x,t)\propto\sigma_0 e^{iqx}e^{-D_Lq^2t}, \tag{5}$$

where x is directed parallel to the cuvette wall. Bragg diffracting a second laser beam (HeNe, $\lambda=633$ nm) off the grid one can trace its decay. The intensity $I_D(t)$ detected by a photodiode can be fitted to the function

$$I_D(t)=[a\cdot f_{DYE}(t)e^{-D_Lq^2t}+b]^2+c, \tag{6}$$

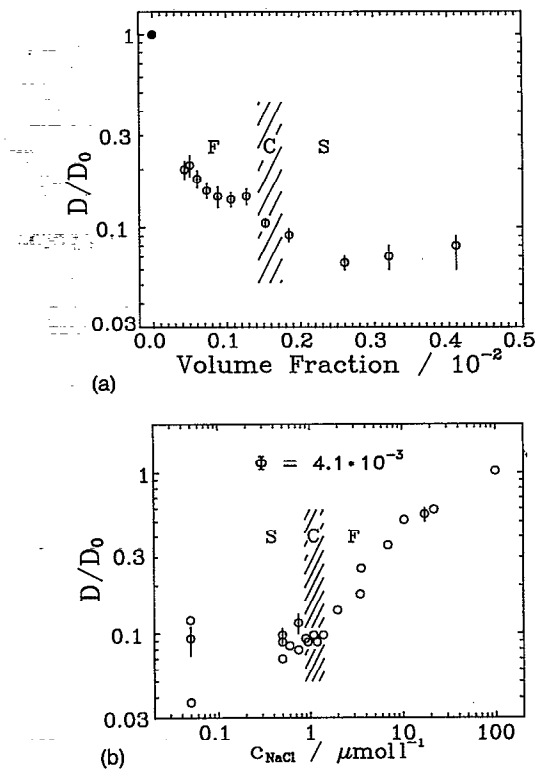

FIG. 2. The self-diffusion coefficient, normalized to the free diffusion coefficient D_0 (a) as a function of volume fraction ϕ in a deionized suspension (b) as a function of salt concentration c_s at constant volume fraction. The coexistence regime between the fluid and solid equilibrium phase is included in both plots. The measurements were always taken in fluid phases, either in equilibrium or in nonequilibrium, which may be called a supercooled fluid.

where the first term of the sum in the parentheses is due to the diffracted beam, b and c are coherent and incoherent background terms[35] differing for each measurement; $f_{DYE}(t)$ is the separately measured relaxation function of the dye. By varying θ and thus q the self-diffusion coefficient D_L can be reliably extracted.

The cylindrical measuring volume of diameter ~ 1 mm is perpendicular to the cell wall. For each measurement up to 20 runs are performed at different spots in the cell and the signals are accumulated.

III. RESULTS

A. Diffusion in equilibrium and in metastable fluid states

As mentioned above the suspension is prepared by continuous deionization, which leaves the system always in a disordered, fluidlike state when it is turned off. This state is either the thermodynamic equilibrium state (fluid) where the free energy is at its minimum, or an nonequilibrium state (supercooled fluid) which is metastable (depending on the relative amount of thermal energy and interaction energy respectively).

Figure 2 shows the first systematic measurements of the diffusion coefficient both in the equilibrium and the nonequilibrium fluid state at different volume fractions and salt concentrations. In Fig. 2(a) the particle concentration

is varied over 1 order of magnitude, i.e., the volume fraction ranges between $\phi=0.0004$ and $\phi=0.0041$ while the suspension stays completely deionized. In Fig. 2(b) the salt concentration is gradually tuned between $c_s<10^{-7}$ mol l^{-1} (complete deionization) and $c_s=10^{-4}$ mol l^{-1} at a constant volume fraction of $\phi=0.0041$.

The diffusion coefficients which are presented in Fig. 2 were all measured in a disordered state (fluid or supercooled fluid) irrespective of the corresponding equilibrium phase. In both plots these equilibrium phases are labeled: **F** (fluid), **C** (coexistence), and **S** (solid). They were determined by static light scattering after the FRS measurements were completed and the equilibrium state was reached. Note that in both cases, i.e., by varying either volume fraction or salt concentration, one observes a coexistence regime rather than a sharp transition from the liquid to the crystalline phase.

The region **F** where the equilibrium state is fluid covers the whole range from very weak interaction to the onset of crystallization. The diffusion coefficient varies by one order of magnitude up to this point in both plots. These data compare well to measurements of Dozier.[14]

As we here were interested in diffusion in the homogeneous fluid state only, the progress of crystallization in the coexistence region **C** was monitored by static light scattering and the measurements presented in this chapter were made before the fraction of crystalline phase reached 10%. No density differences were detected between solid and fluid phases within the experimental error of 2%. Under these conditions we can savely state that over each of the examined coexistence regimes the diffusion coefficient in the shearmolten fluid phase is of the order of $D_L=0.10(1)D_0$. Further measurements at coexistence with $\phi=0.0035$ and $c_s=0.95$ μmol l^{-1} give $D_L/D_0=0.095(1)$. We note that within experimental error no systematic variation of D_L/D_0 over this narrow range of coexistence could be traced. However, it is most remarkable that the absolute value of D_L/D_0 at coexistence seems to be a fixed value [$D_L/D_0=0.10(1)$], independent of salt and particle concentration. Brownian dynamics simulations on interacting colloidal spheres strongly suggest that this is in effect a universal dynamical criterium for fluid–solid phase transitions in Brownian systems.[29] That is, the criterion is valid for spheres interacting via hard-sphere, Coulomb, and screened Coulomb potentials. Hydrodynamic interaction can be included by means of the scaling law proposed by Medina-Noyola.[6] Since for vanishing viscosity the velocity autocorrelation function decays mainly by direct particle–particle interaction, the concept of D_0 becomes invalid. There will, of course, be no such criterion for Newtonian fluids, where there is no viscous suspension medium.

In the shear molten region **S** crystallization progresses faster with strength of interaction increasing.[16] For most of the measurements heterogeneously nucleated wall crystals still grow sufficiently slowly to complete measurements on the fluid without interference of FRS signals stemming from the crystals. However, in the region of highest volume fractions and lowest salt concentration additional homogeneous nucleation occurs. In contrast to the fixed epitactic wall crystal the existence of many fine grained bulk crystals, embedded in the fluid phase, introduces additional nondiffusive modes of grid decay. As crystallization progresses uncertainties are added to the FRS signal. Therefore the measurement is confined to the short period of time after the shearing is stopped and before the amount of solid phase has reached 10%–20%. In this case remaining convection may have influenced the experiment. However we estimate diffusion coefficients to be at most 20% to high.

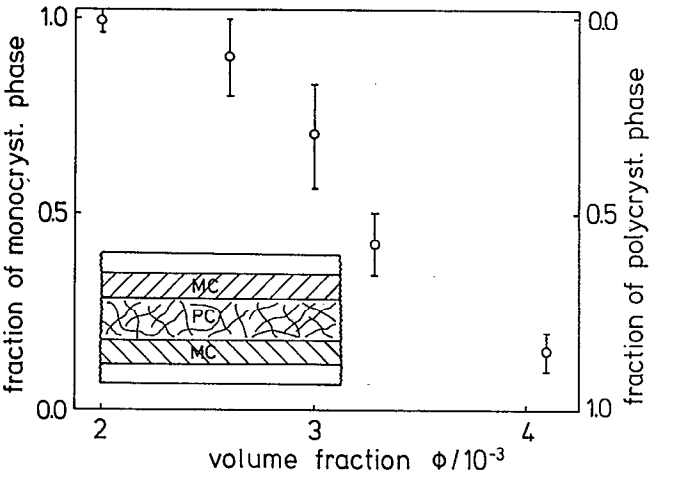

FIG. 3. Relative volumes of mono- and polycrystalline phases in the measuring cell grown from a relaxed suspension after shear had been applied. In a fully deionized suspension heterogenously nucleated, purely monocrystalline samples may be grown at volume fractions between $\phi=0.002$ and $\phi=0.0025$. At higher volume fractions stronger interactions lead to homogenously nucleated polycrystallites. The inset shows the spatial arrangement of the phases in the flat measuring cell. The data on the volume fractions were obtained by static light scattering in a flat cell after equilibrium in crystalline growth was reached. The crystallization processed in a steadily sheared suspension, in nonsteadily sheared suspensions the amount of polycrystalline phase was increased.

For the shear molten region we observe a continued, albeit much smaller decrease of D_L while the strength of interaction is further increased. The decrease of D_L with increasing interaction strength in fact is monotonous over the whole range of accessible suspension parameters; i.e., in our measurements we observe no sudden changes in D_L at the equilibrium phase boundaries.[38] This indicates that the shear molten nonequilibrium fluid indeed shows strong analogies to an atomic supercooled fluid.

B. Diffusion in crystalline phases

As mentioned above monocrystals may be grown after steadily shearing the suspension while polycrystalline samples evolve from nonsteadily sheared suspensions. However, at strong interactions homogeneous nucleation cannot be suppressed and the growth of the monocrystals is disturbed by this nucleation which leads to a coexistence between two monocrystals grown on the walls and small polycrystallites in the middle of the cell. For more clarity we sketch in Fig. 3 the relative amount of different morphologies as a function of volume fraction at $c_s=0$, which

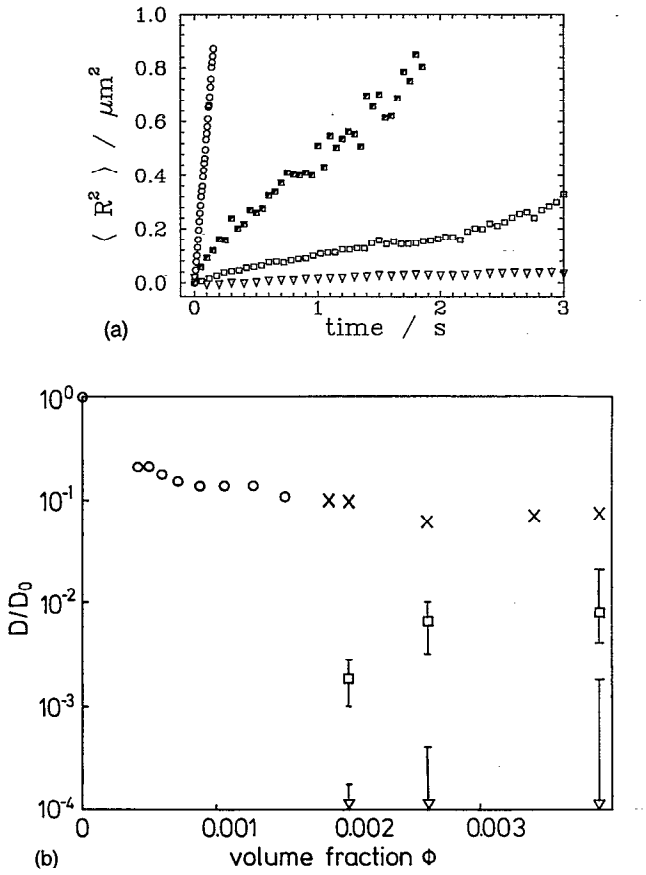

FIG. 4. Comparison of self-diffusional behavior in different phases of completely deionized systems. (○) fluid phase; (*) supercooled phase; (□) polycrystal; (▽) monocrystal. (a) Mean square displacement as a function of time. (ϕ=0.0026, □ was measured in a polycrystal at ϕ=0.0041.) (b) Diffusion coefficients at different volume fractions.

we observed with our cell geometry after constant shear. The amount of the monocrystalline phase was measured by static light scattering. Note that at highest examined volume fraction of 0.0041 the fraction of polycrystalline phase reaches 80%. Even larger amounts in polycrystalline phase are accessible by changing the shear process as described in the experimental section of the paper.

The results of self-diffusion measurements on crystalline samples are shown in Fig. 4 which also includes the data on fluid and shear molten samples for comparison. All data on the solid phases were taken after the equilibrium state was reached. The time dependence of the mean square displacement $\langle R^2 \rangle$ for four single measurements is shown in Fig. 4(a). Strictly monoexponential decays of the FRS signal are found not only in the fluid case but also for a number of polycrystalline samples. Therefore, $\langle R^2 \rangle$ is linear in time in these cases. Some of the polycrystalline samples, however, are characterized by non monoexponential decays. Their data are not shown in Fig. 4(a). The diffusion coefficients could however be extracted by weighted averaging. Furthermore at constant suspension parameters individual samples show different diffusion coefficients. For the monocrystalline samples the change in $\langle R^2 \rangle$ is in the order of the experimental error because dye relaxation dominates the FRS signal.

The normalized diffusion coefficients are compared in Fig. 4(b) for all morphologies investigated. For the monocrystals we are only able to estimate upper limits for D_L. For polycrystalline material the necessary process of averaging significantly enlarges the error bars shown in Fig. 4(b), although the errors of a single experiment are still as small as in the fluid cases.

In polycrystalline samples D_L is over one order in magnitude smaller than in the corresponding shear molten fluid. Similar differences where also found by other groups for high ϕ—high c_s—systems.[12,39] Compared to metallic systems this maximum difference of only 2 orders of magnitude between fluid phase and polycrystalline phase is extremely small. However, we note that a spherical crystal of 1 mm diameter contains only 2×10^9 particles, whereas an equally sized copper grain carries 1×10^{20} Cu atoms. Thus we are actually on a nanocrystalline[40] rather than on a polycrystalline scale.

For the reasons indicated above we cannot yet trace a systematic dependence of D on ϕ in monocrystals. In the polycrystalline phase for the first time such a dependence is well detectable. Following the arguments given above for the fluid phase, we should expect that D decreases with increasing strength of interaction, i.e., volume fraction. The experimental data seem to indicate the opposite behavior. However as discussed above also the morphology of the sample is strongly influenced by the strength of interaction. For the samples investigated here the size of crystallites decreases from roughly 1 mm at ϕ=0.002 to less than 0.1 mm at ϕ=0.0041. With decreasing grain size the volume occupied by grain boundaries is enlarged. In addition also the number of defects might be increased. As self-diffusion inside the grains is considerably slower than in the grain boundaries there should be a clear dependence of D_L on the grain size. This means that the mean value of D_L should increase with decreasing grain size. Indeed this dependence has long been verified for metallic and ionic systems.[41]

A number of theoretical descriptions of grain boundary diffusion in poly- and nanocrystalline material are available.[40] Still the set of data presented here is too small to advance from qualitative analogies to a rigorous quantitative treatment.

C. Diffusion in equilibrium coexistence

In the measurements presented so far diffusion was accurately measurable in single phase samples. It is not intuitively clear that this is also true for coexisting phases, since then we would expect more complicated FRS signals. With our preparational setup a two phase system is given for the fluid/solid coexistence. Over a narrow range of salt concentrations we observe that the fully grown wall crystals reproducibly occupy only a fraction of the sample volume. This situation is of special interest as both data on the diffusional behavior of the two phase region compared to

TABLE I. Characterization of samples with $\phi=0.0041$ of 102 nm spheres at low salt concentrations.

#	c_s μmol l^{-1}	Morph.	Crystal vol.	D_C/D_0	D_F/D_0	D_{SM}/D_0
1	<0.1	PC	>0.95	0.01		0.09(2)
2	0.5	MC	>0.95	<0.002		0.08(1)
3	0.6	MC	>0.95	<0.002		0.085(10)
4	0.85	F/MC	0.8(1)	<0.003	0.09(3)	0.14(2)
5	1.1	F/MC	0.67(5)	<0.003	0.09(3)	0.097(10)
6	1.2	F/MC	0.56(5)	<0.004	0.11(2)	0.090(10)
7	1.4	F/MC	0.04(2)	~0.0	0.097(10)	0.097(10)
8	2.0	F	<0.01		0.14(1)	0.14(1)

single phase material and on the relative amount of these phases are not yet available.

In the coexistence region we find the FRS signal to be the sum of two single exponentials. The two decay constants are different by more than two orders of magnitude and may therefore safely be separated. The faster diffusing compound can be related to the fluid phase since it has the appropriate time constant. The slow component is identified with the monocrystalline phase.

We summarize our results in Table I. Within experimental error the diffusion coefficients stay constant and equal the values of pure fluid and pure monocrystal respectively. Table I also contains the data on the relative amount of the two phases, derived from the amplitude factors a [cf. Eq. (6)] checked by the Bragg scattered intensities. For salt concentrations $0.8\ \mu\text{mol}\,\text{l}^{-1} < c_s < 1.4\ \mu\text{mol}\,\text{l}^{-1}$ we unequivocally detect coexistence. The relative amount of solid phase decreases with increasing c_s.

IV. CONCLUSIONS

Different phases of ordered colloids were reproducibly prepared, and the long time self-diffusion coefficient was measured in these phases.

—In the fluid and supercooled phase we saw a continous decrease of the self-diffusion coefficient with increasing interaction. D_L/D_0 is close to 0.10 at the equilibrium phase boundary.

—The monocrystalline phase did not exhibit a measurable diffusion, which means that diffusion is at least four orders of magnitude slower than in the fluid phase.

—In polycrystalline phase we measured self-diffusion coefficients only about two orders of magnitude lower than in the fluid phase. A tendency of increased grain boundary diffusion with decreasing crystallite size was observed.

—FRS was for the first time used to simultaneously measure diffusion in two coexisting phases, namely at the equilibrium coexistence of solid and fluid, which was found in a narrow region of preparation parameters. The diffusion coefficient in the coexisting phases was not found to differ from the values found in the pure fluid and the pure monocrystal at equal suspension parameters.

ACKNOWLEDGMENTS

We thank the group of R. Weber for their help in particle characterization measurements and H. Löwen, K. Schätzel, and M. Würth for helpful discussions. This work was supported by the DFG (SFB 306).

[1] P. N. Pusey, *Liquids, Freezing and the Glass Transition*, edited by D. Levesque, J.-P. Hansen, and J. Zinn-Justin (Elsevier, Amsterdam, 1990).
[2] H. Lekkerkerker, *Structure and Dynamics of Strongly Interacting Colloids and Supramolecular Aggregates in Solution*, edited by S.-H. Chen, J. S. Huang, and P. Tartaglia, NATO ASI Series (Kluwer, Dordrecht, 1992).
[3] G. K. Batchelor, J. Fluid Mech. **131**, 155 (1983), and references therein.
[4] C. W. J. Beenakker and P. Mazur, Physica A **126**, 349 (1984).
[5] B. Cichocki and B. U. Felderhof, J. Chem. Phys. **89**, 1049 (1988); B. Cichocki and B. U. Felderhof, *ibid.* **89**, 3705 (1988).
[6] M. Medina-Noyola, Phys. Rev. Lett. **60**, 2705 (1988).
[7] M. M. Kops-Werkhoven and H. M. Fijnaut, J. Chem. Phys. **77**, 2242 (1982); M. M. Kops-Werkhoven, C. Pathmamanoharan, A. Vrij, and H. M. Fijnaut, *ibid.* **77**, 5913 (1982).
[8] A. van Veluwen, H. N. W. Lekkerkerker, C. G. de Kruif, and A. Vrij, J. Chem. Phys. **87**, 4873 (1987).
[9] R. H. Ottewil and N. S. J. Williams, Nature (London) **325**, 232 (1987).
[10] W. van Megen and S. M. Underwood, J. Chem. Phys. **91**, 552 (1989).
[11] R. Piazza, V. Degiorgio, M. Corti, and J. Stavans, Phys. Rev. B **42**, 4885 (1990).
[12] A. van Blaaderen, J. Peetermans, G. Maret, and J. K. G. Dhont, J. Chem. Phys. **96**, 4591 (1992).
[13] G. Nägele, M. Medina-Noyola, R. Klein, and J. R. Arauz-Lara, Physica A **149**, 123 (1988).
[14] W. D. Dozier and P. M. Chaikin, J. Phys. (Paris) **46**-C.3, 165 (1985).
[15] T. Palberg, W. Härtl, H. Versmold, M. Würth, and E. Simnacher, J. Phys. Chem. **96**, 8180 (1992).
[16] M. Würth, T. Palberg, and P. Leiderer (in preparation).
[17] H. O. Moser, O. Fromhein, F. Herrman, and H. Versmold, J. Phys. Chem. **92**, 6723 (1988).
[18] S. Alexander, P. M. Chaikin, P. Grant, G. J. Morales, P. Pincus, and D. Hone, J. Chem. Phys. **80**, 5776 (1984).
[19] W. Härtl and H. Versmold, J. Chem. Phys. **88**, 7157 (1988).
[20] L. P. Voegtli and C. F. Zukowski IV, J. Colloid Interf. Sci. **141**, 79 (1991).
[21] M. O. Robbins, K. Kremer, and G. S. Grest, J. Chem. Phys. **88**, 3286 (1988).
[22] E. J. Meijer and D. Frenkel, J. Chem. Phys. **94**, 2269 (1991).
[23] E. B. Sirota, H. D. Ou-Yang, S. K. Sinha, P. M. Chaikin, J. D. Axe, and Y. Fuji, Phys. Rev. Lett. **62**, 1524 (1989).
[24] Y. Monovoukas and A. P. Gast, J. Coll. Interface Sci. **128**, 533 (1989).
[25] A. J. Sood, Solid State Phys. **45**, 1 (1990).
[26] Phase Transitions **24**(2–4) (1990).
[27] R. Krause, G. Nägele, D. Karrer, J. Schneider, R. Klein, and R. Weber, Physica A **153**, 400 (1988).
[28] W. Dozier, Thesis, University of California, Los Angeles, 1986.
[29] H. Löwen, T. Palberg, and R. Simon; Phys. Rev. Lett. **70**, 1557 (1993).
[30] Due to the extremely low values of the elastic constants, which scale with the particle density and therefore are about 12 orders of magnitudes lower than in atomic systems, a colloidal solid can easily be molten by applying a shear stress (Refs. 31 and 32).
[31] B. J. Ackerson and N. A. Clark, Phys. Rev. A **30**, 906 (1984).
[32] D. A. Weitz, W. D. Dozier, P. M. Chaikin, J. Phys. (Paris) **46**-C.3, 257 (1985).
[33] D. J. W. Aastuen, N. A. Clark, L. K. Cotter, and B. J. Ackerson, Phys. Rev. Lett. **57**, 1733 (1987).
[34] D. W. Pohl, S. E. Schwarz, and V. Irniger, Phys. Rev. Lett. **31**, 32 (1973).
[35] H. Hervet, W. Urbach, and F. Rondelez, J. Chem. Phys. **68**, 2725 (1978); F. Rondelez, W. Urbach, and H. Hervet, Phys. Rev. Lett. **41**, 1058 (1978).
[36] J. Coutandin, H. Sillescu, and R. Voelkel, Makromol. Chem.-Rapid Commun. **3**, 649 (1982).

[37] T. Palberg, R. Simon, and P. Leiderer, Progr. Colloid Polym. Sci. **84**, 397 (1991).

[38] The kink in the measured curve of Fig. 2(a) at $\phi=0.0014$ just below the equilibrium phase transition is presently interpreted as a fluctuation within statistical error. More detailed investigations in the vicinity of the phase boundary are in progress.

[39] R. Piazza and V. Degiorgio, Phys. Rev. Lett. **67**, 3869 (1991).

[40] J. Horváth, R. Birringer, and H. Gleiter, Solid State Commun. **62**, 319 (1987); A. Atkinson and R. I. Taylor, Philos. Mag. A **43**, 979 (1981).

[41] J-F. Laurent and J. Bérnard, J. Phys. Chem. Solids **7**, 218 (1958); L. G. Harrison, Trans. Faraday Soc. **57**, 1191 (1961).